Relative stability of Cu, Ag, and Pt at high pressures and temperatures from *ab initio* calculations

N. A. Smirnov*
FSUE RFNC-VNIITF named after academ. E. I. Zababakhin, 456770, Snezhinsk, Russia

(Received 25 October 2020; revised 11 February 2021; accepted 15 February 2021; published 23 February 2021)

The paper presents *ab initio* studies into the relative stability of the crystalline structures of copper, silver, and platinum up to high pressures at $T \geqslant 0$ K. Our calculations in quasiharmonic approximation suggest that not the fcc structure of Cu and Ag, but the body-centered cubic one, is thermodynamically most favorable at $P \gtrsim 100$ GPa and $T > 3$ kK. The shock Hugoniot of Cu and Ag crosses the fcc-bcc phase boundary and the calculated transition pressures agree well with the result of recent laser shock experiments by Sharma *et al.* The advantage of the bcc structure comes from its softer low-frequency phonon modes and the smaller contribution of lattice vibrations to free energy at high temperatures, as compared to close-packed structures. The compression of platinum crystal also causes the fcc → bcc transition but at much higher pressures, $P > 1.4$ TPa.

DOI: 10.1103/PhysRevB.103.064107

I. INTRODUCTION

Due to advances in the nanosecond x-ray spectroscopy technique, a number of experimental studies have been taken in recent years to investigate structural changes which occur in materials under shock compression. The most recent of them were devoted to the detection of phase transitions in such metals as copper, silver, gold, and platinum [1–4]. They showed the structural transformation from the face-centered cubic lattice to the body-centered one to occur in Cu, Ag, and Au before the onset of melting. That was quite an unexpected result because earlier shock experiments did not show any anomalies pointing to the existence of the phase transition [5–10]. Static diamond anvil-cell measurements [11–16] also did not detect the fcc → bcc transition.

In turn, theoretical results obtained for Cu and Ag from first principles show that the structural transition to the bcc phase does not occur in these metals at $T = 0$ K at least to pressures $P \approx 100$ TPa [17,18]. Thus far no attempts have been made to study the possibility of the fcc → bcc transition in compressed copper and silver at high temperatures. For gold, several structural changes were predicted to occur under pressure [12,19,20]. Moreover, it was shown in Ref. [20] that the fcc → bcc transition must occur in Au under high pressures and temperatures which was later detected in shock experiments [1,2].

The structural stability of platinum under high P and T is studied in at least two papers [21,22]. The authors of Ref. [21] use first-principles molecular dynamics (DFT-MD) calculations to predict the existence of the randomly disordered hexagonal close-packed structure (rhcp) at pressures above 40 GPa and temperatures >3 kK. But later, in laser-heated diamond anvil-cell measurements [22] and shock-wave experiments [3], no phase transitions were detected at least to $P \approx 380$ GPa. On the other hand, as shown in Ref. [23], the bcc phase of Pt becomes more energetically favorable than fcc at a pressure of about 2 TPa and zero temperature.

The authors of experimental works [3,4] suppose the mechanism of plastic deformation plays an important role in the fcc → bcc transition for Cu, Ag, and Au metals. Under shock compression, abundance of stacking faults form in them shortly before the structural transition starts and these stacking faults may facilitate structural changes. No such growth of stacking faults is observed in platinum and the transition does not occur [3]. However, it should be noted that in dynamic ramp experiments [10] for copper, no structural changes were observed at least to 1.15 TPa. From sound velocity data the authors of Ref. [10] suppose that no structural changes might occur up to $P = 2.3$ TPa. Temperatures in ramp experiments are generally much lower than in conventional shock experiments and the P-T path of interest is usually quite close to the principal isentrope [24]. Thus, the question of where the place of the fcc → bcc transition is on the phase diagram of copper still remains opened.

II. DETAILS OF CALCULATIONS

In order to see the particular features of structural changes in Cu, Ag, and Pt we study their structural phase stability under high pressures and temperatures up to the melting point. In this work we used for calculations the all-electron full-potential linear MT-orbital method FP-LMTO [25]. Its internal parameters were adjusted so as to ensure required accuracy (∼0.1 mRy/atom) [20]. Considered are the fcc, bcc, hcp, and dhcp structures as the most probable candidates for the high pressure phase of noble metals [12,19,20]. The following atomic levels were taken as valence: $3s$, $3p$, $3d$, and $4s$ for copper, $4s$, $4p$, $4d$, and $5s$ for silver, and $5s$, $5p$, $4f$, and $5d$ for platinum. Calculations were done in the scalar-relativistic approximation with gradient (GGA) exchange-correlation (XC) functionals [26,27] for Cu, and PBEsol [28] for Ag and Pt. These functionals have earlier demonstrated good accuracy in the calculation of copper,

*nasmirnov@vniitf.ru

silver, and platinum properties [13,23,29]. The basis set was limited to the moment $l^b_{\max} = 4$. Charge density and potential expansions in terms of spherical harmonics were done to $l^w_{\max} = 7$. The improved tetrahedron method [30] was used for integration over the Brillouin zone. The meshes in **k** space measured $30 \times 30 \times 30$ for the cubic structures, and $30 \times 30 \times 18$ and $30 \times 30 \times 15$ for the hcp and dhcp phases, respectively. The phonon spectra were calculated with linear response theory implemented in the FP-LMTO code [25]. Phonon frequencies were determined using meshes of **q** points which measured $10 \times 10 \times 10$ for the cubic structures, and $10 \times 10 \times 6$ and $10 \times 10 \times 5$ for hcp and dhcp, respectively. The parameter c/a for hexagonal lattices was always optimized.

The energy convergence criterion that defines the number of iterations of the self-consistent loop was taken to be 10^{-3} mRy/cell. The pressure versus volume dependence was calculated by differentiation of an analytical expression which approximated the energy-volume dependence. The formula by Parsafar and Mason [31] was used for this approximation. The dependence of internal energy versus relative specific volume V/V_0 (V_0 standing for specific volume under ambient conditions) was calculated in the interval from 1.05 to 0.3 at a step of 0.05. The phonon spectra were calculated at a step of 0.1. The contribution of lattice vibrations to free and internal energies were determined in quasiharmonic approximation [32] with use of the calculated phonon spectra. The value of free (internal) energy for each V and T was determined by adding the thermal contribution of lattice vibrations to cold energies. The Gibbs potential was calculated with the known formula $G = F + PV$. To calculate the principal isentrope, we determined the value of entropy $TS_{300} = E - F$ under ambient conditions. The corresponding isentrope curve was determined from the condition $S[V(P,T),T] = S_{300}$ for specified V and T. The well-known Lindemann criterion was used to evaluate the melting curve. The procedure of its calculation is described in Ref. [23].

III. RESULTS AND DISCUSSION

Figure 1 shows the Gibbs potential differences of considered structures at zero temperature for the three metals. The energies of fcc and dhcp copper are seen to be very close but calculations show that the contribution of lattice vibration to free energy for dhcp is a bit higher than for fcc and the structural transition fcc → dhcp will not occur. Thus, at $T = 0$ K, fcc Cu is very likely to remain most favorable up to very high pressures which agrees with other calculations [12,17]. Note that the bcc structure is energetically much less favorable than the close-packed phases at zero temperature.

For silver the pattern is somewhat changed (see the middle panel of Fig. 1). Below $P = 2.5$ TPa, two structural transitions occur: the first, fcc → dhcp, at a pressure of about 0.6 TPa, and the second, dhcp → hcp, at $P > 2$ TPa. Like in the case of Cu and Au [20], the difference between the energies of the close-packed phases is small and calculated results are very sensitive to parameters of the calculation method. The energy of the bcc phase is also markedly higher than those of the close-packed structures at $T = 0$ K. These results agree quite well with other calculations [12,18]. In particular, it is shown

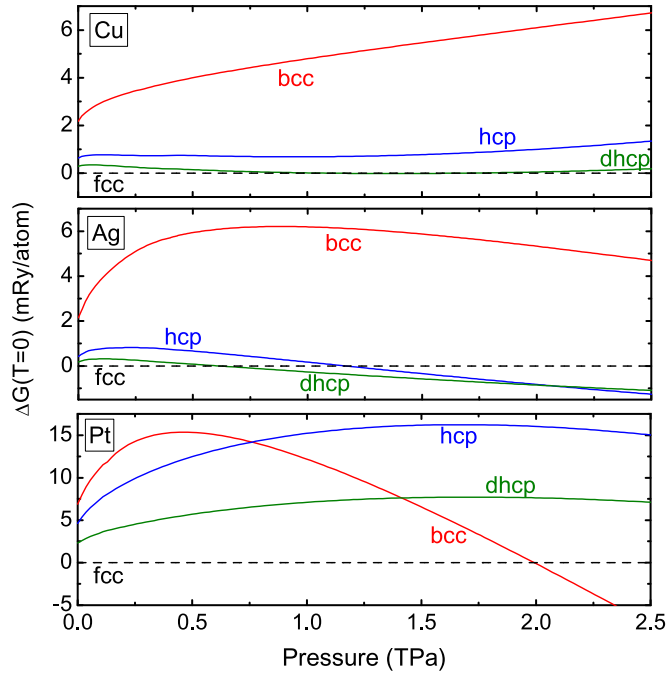

FIG. 1. Calculated Gibbs potential differences ΔG for the considered structures of Cu, Ag, and Pt in the pressure range up to 2.5 TPa at $T = 0$ K (relative to G for fcc).

in Ref. [18] that at $P > 0.5$ TPa the transition to a hexagonal close-packed phase may occur in silver.

The lower panel of Fig. 1 shows the thermodynamic potential differences ΔG for platinum. As seen from the figure, the structural fcc → bcc transition must occur in Pt at $P \approx 2.0$ TPa. One can also see that in considered range of pressures, the scale of changes in the energy of the close-packed phases of Pt is much larger than in the other metals. So, among the metals we are considering, only platinum transforms from fcc to bcc at $T = 0$ K and $P \leqslant 2.5$ TPa. But it will be shown below that the situation strongly changes with the increasing temperature.

Figure 2 shows specific energy (E_{tot}) of the copper lattice versus lattice parameter c/a for different relative volumes V/V_0 at $T = 0$ K. It is seen from the figure that at $V/V_0 = 1$ the bcc structure is dynamically unstable which agrees well with other calculations [33]. As compression increases ($V/V_0 \lesssim 0.8$, $P \gtrsim 60$ GPa), the minimum corresponding to the bcc structure of copper appears in the $E_{\text{tot}}(c/a)$ curve. In turn, the fcc phase remains stable and the energy difference between the cubic phases gradually increases. As shown by calculations, the situation does not change up to very high pressures ($P > 2.5$ TPa). The bcc structure remains metastable in a wide range of compressions. A similar behavior is observed for silver, whose bcc phase also becomes dynamically stable at $V/V_0 \lesssim 0.8$ and remains metastable up to high pressures. The behavior of platinum is a bit different. Below 1.4 TPa ($V/V_0 \approx 0.47$) at $T = 0$ K, its bcc phase is dynamically unstable and stabilizes only at higher pressures.

Now look at the phonon spectra of Cu and Ag crystals for different structures under pressure. Figure 3 compares the phonon densities of states (PDOS) of the phases under

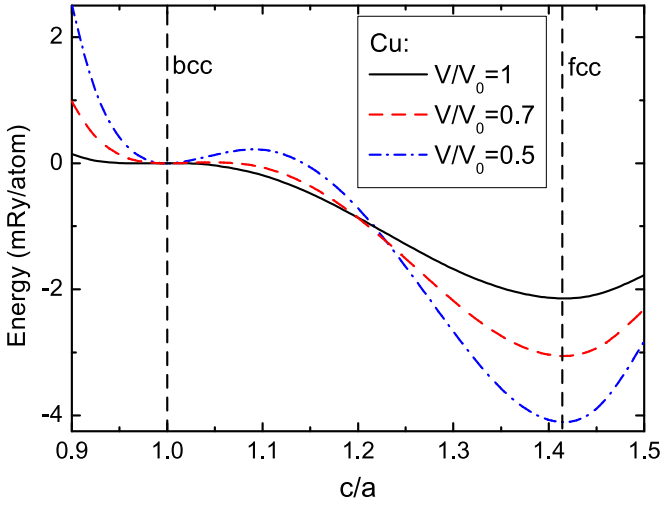

FIG. 2. Internal energy versus c/a ratio (Bain path) at $T = 0$ K for several compressions of copper.

consideration at $V/V_0 = 0.6$. Calculations show that the low-frequency phonon modes of bcc Cu and Ag are markedly softer than those of the close-packed phases (Fig. 3). The first low-frequency maximum related to the transverse phonon modes is seen to be noticeably shifted to low frequencies. Therefore the contribution of thermal lattice vibrations to the free energy of the bcc phase is lower than that of the other structures. This behavior does not change up to high pressures (>2 TPa) and cardinally affects the phase diagram of Cu and Ag.

For platinum the situation is a bit different. The left panel of Fig. 4 shows the phonon densities of states for four platinum structures at a pressure of about 1.65 TPa ($V/V_0 = 0.45$), i.e., before the structural fcc → bcc transition occurs. Reminder that at $V/V_0 > 0.47$ and $T = 0$, bcc Pt is dynamically unstable. On whole, the pattern is similar to what was demonstrated for copper and silver. The bcc phase has the softer low-frequency phonon modes and the contribution of its phonons to the free energy of the system is lower compared to fcc. But with the increasing compression the situation rapidly changes so that almost immediately after the fcc → bcc

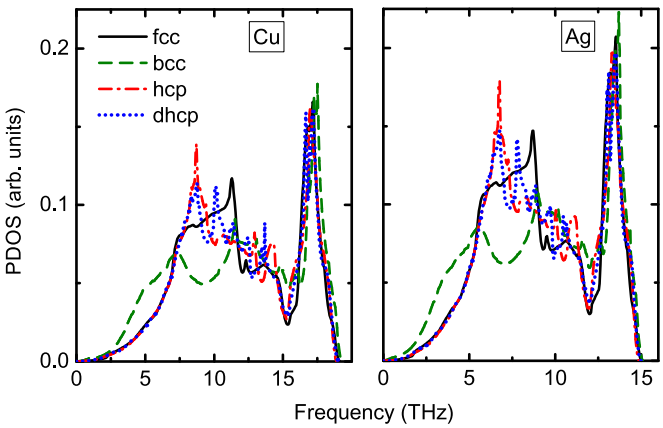

FIG. 3. Phonon densities of states for the considered structures of Cu and Ag at $V/V_0 = 0.6$ and $T = 0$ K.

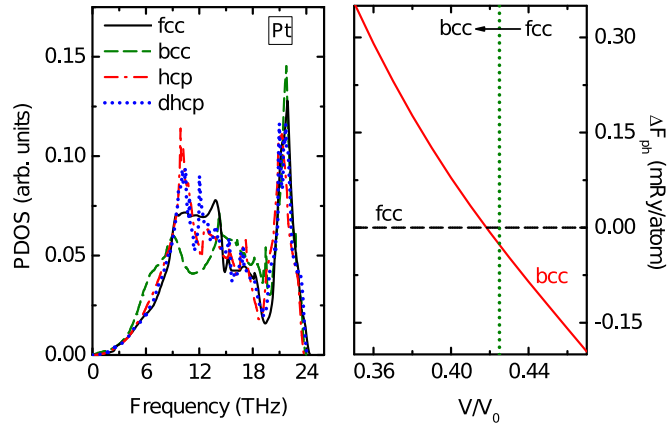

FIG. 4. Left panel: Phonon densities of states for the considered structures of Pt at $V/V_0 = 0.45$. Right panel: Free energy difference of the phonon gas (red line) at $T = 300$ K for bcc and fcc Pt near the fcc → bcc transition (green dotted line).

transition the contribution of lattice vibrations to free energy for bcc becomes larger (see the right panel of Fig. 4). In the cases of copper and silver, this does not occur at least to $V/V_0 \approx 0.32$ ($P \approx 3$ TPa).

Figures 5 and 6 show the phase diagrams of copper and silver calculated in this work. It is seen that the melting curves obtained with the Lindemann criterion agree well with available experimental data [34–36] (see Fig. 5 and the inset in Fig. 6). One can also see that the fcc → bcc transition occurs in both metals above some pressure as temperature increases. The existence of the fcc structure on the phase diagrams of Cu and Ag is limited from above by temperatures in a few thousand Kelvin. The softer bcc phase appears due to its dynamical stabilization with the growing P. The transition occurs because of the higher entropy and the lower contribution of lattice vibrations to the free energy of the bcc

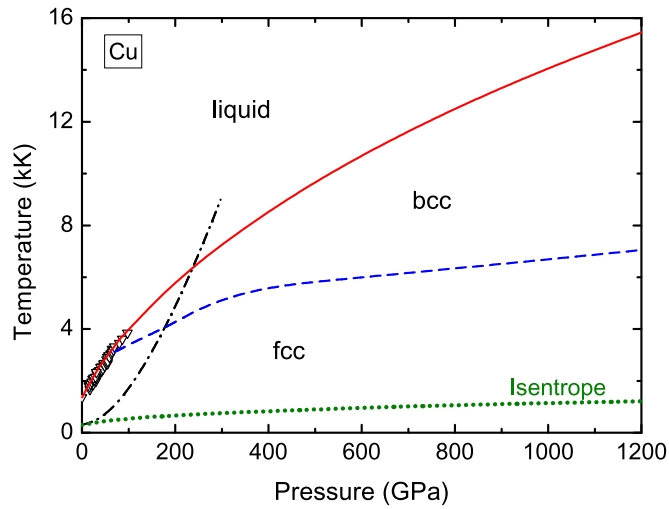

FIG. 5. Phase diagram of copper. The lines show calculated results: the melting curve (the solid line), the fcc-bcc phase boundary (the dashed one), fcc Cu Hugoniot (the dash-dotted line), and the principal isentrope (the dotted one). Triangles show points on the experimental melting curve [34].

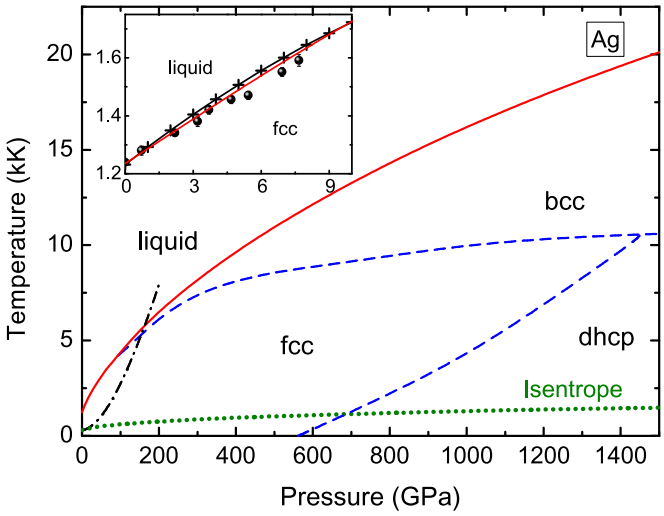

FIG. 6. Phase diagram of silver. Results of calculations designate the same as in Fig. 5. Also shown is the calculated fcc-dhcp phase boundary. The inset shows the melting curve at low P: the line with crosses is experimental results from [35], and the circles show experiment [36].

lattice compared to the other lattices. A similar behavior has recently been detected in compressed ($P > 150$ GPa) tin and lead crystals [24] where the hcp lattice which is more energetically favorable at $T = 0$ K becomes less favorable than the softer bcc lattice as temperature increases. In addition to the fcc → bcc transition, one more structural transformation, fcc → dhcp, exists in silver at relatively low temperatures (see Fig. 6). The boundary between these phases has a positive slope and the region where the fcc structure exists increases rather greatly as P and T grow.

Let us look closer into the fcc → bcc transition in Cu and Ag using as an example the dependence of the Gibbs potentials G of these structures versus T and P. Figures 7 and 8 demonstrate their relative difference versus temperature for two characteristic pressures. It is seen that the values of G for

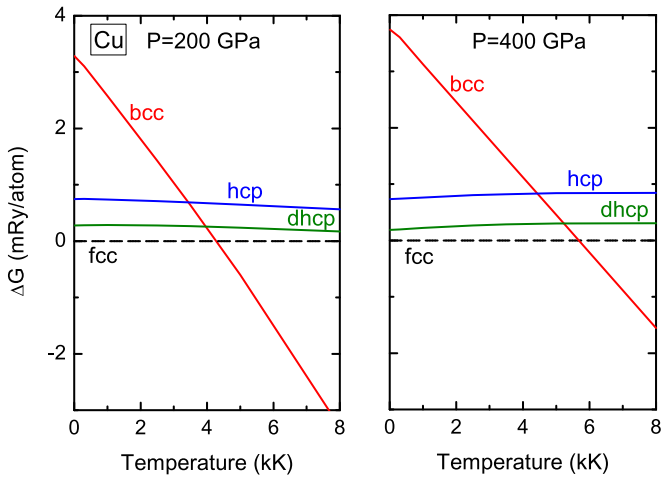

FIG. 7. Gibbs potential difference between the considered copper structures (relative to fcc) versus temperature at pressures 200 GPa (left panel) and 400 GPa (right panel).

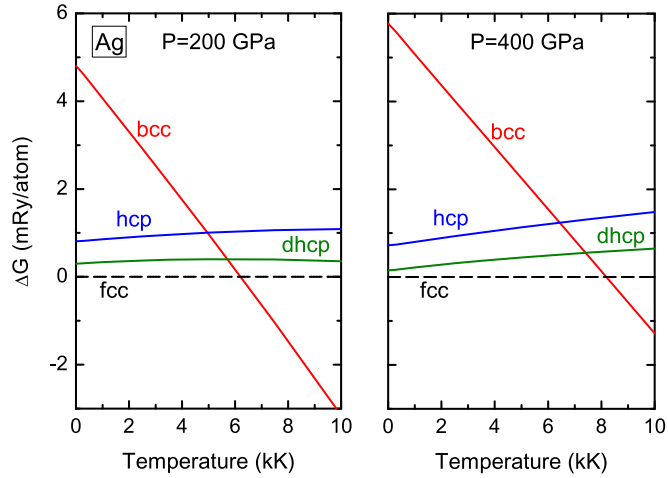

FIG. 8. Gibbs potential difference between the considered silver structures (relative to fcc) versus temperature at pressures 200 GPa (left panel) and 400 GPa (right panel).

the hexagonal structures are rather close to the Gibbs energy of the fcc phase and ΔG weakly changes with the increasing temperature. As a counter to this, the Gibbs potential of the bcc structure gets rapidly smaller than that of the fcc one and the bcc structure becomes energetically more favorable. Here the energy difference is rather large. So, for example, its change by 0.3 mRy/atom (≈4 meV/atom) will shift the fcc-bcc phase boundary by no more than about 300 K.

It is also seen from Figs. 5 and 6 that the fcc-bcc phase boundary crosses the shock adiabat both in copper and in silver. The transition pressures on the Hugoniot are calculated to be 177 and 153 GPa for Cu and Ag, respectively, which agree well with ∼180 (Cu) and 144–158 (Ag) GPa obtained in experiments [3,4]. Thus, from the thermodynamic point of view, it is shown that the fcc → bcc transition may exist on the Hugoniots of these metals. The effect of stacking faults on the parameters of this transition requires further investigation. As seen from Figs. 5 and 6, the calculated fcc-bcc phase boundary runs down below 100 GPa. Unfortunately, in laser-heated diamond anvil-cell experiments [34], the melting of Cu was detected optically and the crystal structure of the melting material at high pressure was assumed to be fcc. Therefore the question of observing the fcc → bcc structural transition in static experiments at $P < 100$ GPa and high temperatures remains undetermined at the moment. As shown by calculations, the closer to the dynamic stability boundary, the sharper is the increase of the error from the use of the quasiharmonic approximation for high temperatures (see, for example, [37]). For more accurate calculation, it is necessary to account for higher order anharmonic effects which can be done with MD modeling. Now, there exist several approaches which use results of *ab initio* calculations [38–43]. As shown in Ref. [43], for many metals including Ag and Cu, the contributions from phonon-phonon interaction and from thermal electron excitation to the Gibbs energy are opposite in sign. For copper, these contributions are approximately equal. It is possible that these contributions will cancel each other, which gives hope for the reliability of the results obtained in the quasiharmonic approximation. Nevertheless the existence of

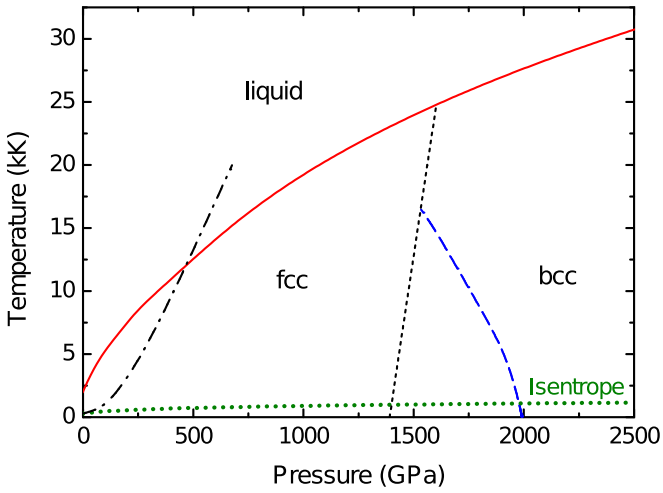

FIG. 9. The calculated phase diagram of platinum. The red line is the melting curve, the black dash-dotted line is the Hugoniot from [23], the green dotted line is the principal isentrope, and the blue dashed line is the fcc-bcc phase boundary. The black short-dashed line shows the dynamic stability boundary of bcc Pt (see the text).

the bcc phase in Cu and Ag at pressures below 100 GPa and high temperatures is still to be proved, though in some cases the accuracy of quasiharmonic calculations at high pressures is quite acceptable [20,24].

In Figs. 5 and 6 one can see the principal isentrope calculated in this work. It runs much lower than the fcc-bcc phase boundary and does not cross it at least to pressures about 2.5 TPa. This explains why the structural transition was not detected in ramp experiments for Cu. According to data from Ref. [10], the experimental P-T path is rather close to the principal isentrope. Calculations suggest that unlike copper, silver may transform into its double hexagonal close-packed phase under quasi-isentropic compression to pressures >600 GPa.

Figure 9 shows the PT diagram of platinum calculated in this work. It is seen that under pressure the region where the fcc phase exists reduces as temperature increases because of its harder low-frequency phonon modes compared to bcc phase (see Fig. 4). Since at $T = 0$ K and $P < 1.4$ TPa the bcc structure is dynamically unstable, there exists a region on the PT diagram where the temperature dependence of the Gibb potential for this phase cannot be determined within the simple quasiharmonic approximation. The short-dashed black line in Fig. 9 shows the boundary of this region. The fcc-bcc phase boundary cannot be extended to the left of it without the phonon-phonon interaction taken into account. It is however clear that the fcc-bcc phase boundary is far from the Hugoniot and, unlike copper and silver, there is no reason for expecting the structural transition to occur in Pt under single compression by shock waves. The fcc → bcc transformation in platinum should be expected to occur at about 2 TPa in ramp experiments, as seen in Fig. 9.

IV. CONCLUSIONS

In conclusion, it has been demonstrated through calculations from first principles that in the Cu and Ag metals at $P \gtrsim 100$ GPa and $T > 3$ kK, there may exist a region where the body-centered cubic phase is thermodynamically more favorable than fcc. The bcc structure thermodynamically stabilizes because its low-frequency phonon modes are softer compared to close-packed phases and, hence, the contribution of lattice vibrations (calculated within quasiharmonic approximation) to free energy is smaller. The shock Hugoniot crosses the fcc-bcc phase boundary both in Cu and in Ag, and the calculated transition pressures agree well with recent shock experimental results [3,4]. Calculations show that under quasi-isentropic compression the experimental P-T path runs below the boundary of the fcc-bcc transition to high pressures. However, in silver the transition to the double hexagonal close-packed phase should be expected at $P > 600$ GPa and relatively low temperatures. In platinum, the fcc → bcc transition should not be expected to occur below 2 TPa at $T \sim 300$ K.

Thus, at least in some noble metals (Cu, Ag, Pt, and Au), at $0.1 \lesssim P \lesssim 2$ TPa and high temperatures, a structural fcc-bcc transition exists. In gold [20] and platinum, the bcc phase is most stable at low temperatures as well. In this context it would be good to test the other noble fcc metals (Rh, Pd, Ir) for their bcc structure stabilization at high P and T. In addition, our evaluations (with the LOVA approximation [44]) show that the transport properties of Cu and Ag markedly change at the phase transition point on the shock adiabat. So the electrical and heat conductivities of the new bcc structure is by about 30% lower that those of the fcc phase.

[1] R. Briggs, F. Coppari, M. G. Gorman, R. F. Smith, S. J. Tracy, A. L. Coleman, A. Fernandez-Panella, M. Millot, J. H. Eggert, and D. E. Fratanduono, Phys. Rev. Lett. **123**, 045701 (2019).
[2] S. M. Sharma, S. J. Turneaure, J. M. Winey, Y. Li, P. Rigg, A. Schuman, N. Sinclair, Y. Toyoda, X. Wang, N. Weir, J. Zhang, and Y. M. Gupta, Phys. Rev. Lett. **123**, 045702 (2019).
[3] S. M. Sharma, S. J. Turneaure, J. M. Winey, and Y. M. Gupta, Phys. Rev. Lett. **124**, 235701 (2020).
[4] S. M. Sharma, S. J. Turneaure, J. M. Winey, and Y. M. Gupta, Phys. Rev. B **102**, 020103(R) (2020).
[5] L. V. Al'tshuler, A. A. Bakanova, I. P. Dudoladov, E. A. Dynin, R. F. Trunin, and B. S. Chekin, J. Appl. Mech. Tech. Phys. **22**, 145 (1981).
[6] D. Hayes, R. S. Hixson, and R. G. McQueen, AIP Conf. Proc. **505**, 483 (2000).
[7] M. Yokoo, N. Kawai, K. G. Nakamura, and K. Kondo, Appl. Phys. Lett. **92**, 051901 (2008).
[8] R. W. Lemke, D. H. Dolan, D. G. Dalton, J. L. Brown, K. Tomlinson, G. R. Robertson, M. D. Knudson, E. Harding, A. E. Mattsson, J. H. Carpenter, R. R. Drake, K. Cochrane, B. E. Blue, A. C. Robinson, and T. R. Mattsson, J. Appl. Phys. **119**, 015904 (2016).
[9] C. A. McCoy, M. D. Knudson, and S. Root, Phys. Rev. B **96**, 174109 (2017).
[10] D. E. Fratanduono, R. F. Smith, S. J. Ali, D. G. Braun, A. Fernandez-Panella, S. Zhang, R. G. Kraus, F. Coppari,

J. M. McNaney, M. C. Marshall, L. E. Kirch, D. C. Swift, M. Millot, J. K. Wicks, and J. H. Eggert, Phys. Rev. Lett. **124**, 015701 (2020).
[11] G. Weck, V. Recoules, J.-A. Queyroux, F. Datchi, J. Bouchet, S. Ninet, G. Garbarino, M. Mezouar, and P. Loubeyre, Phys. Rev. B **101**, 014106 (2020).
[12] L. Dubrovinsky, N. Dubrovinskaia, W. A. Crichton, A. S. Mikhaylushkin, S. I. Simak, I. A. Abrikosov, J. S. de Almeida, R. Ahuja, W. Luo, and B. Johansson, Phys. Rev. Lett. **98**, 045503 (2007) (see also Supplemental Material).
[13] A. Dewaele, M. Torrent, P. Loubeyre, and M. Mezouar, Phys. Rev. B **78**, 104102 (2008).
[14] N. Dubrovinskaia, L. Dubrovinsky N. A. Solopova, A. Abakumov, S. Turner, M. Hanfland, E. Bykova, M. Bykov, C. Prescher, V. B. Prakapenka, S. Petitgirard, I. Chuvashova, B. Gasharova, Y.-L. Mathis, P. Ershov, I. Snigireva, and A. Snigirev, Sci. Adv. **2**, e1600341 (2016).
[15] Y. Ye, V. Prakapenka, Y. Meng, and S.-H. Shim, J. Geophys. Res. Solid Earth **122**, 3450 (2017).
[16] A. Dewaele, P. Loubeyre, F. Occelli, O. Marie, and M. Mezouar, Nat. Commun. **9**, 2913 (2018).
[17] C. W. Greeff, J. C. Boettger, M. J. Graf, and J. D. Johnson, J. Phys. Chem. Solids **67**, 2033 (2006).
[18] J. C. Boettger, Int. J. Quantum Chem. **112**, 3822 (2012).
[19] T. Ishikawa, K. Kato, M. Nomura, N. Suzuki, H. Nagara, and K. Shimizu, Phys. Rev. B **88**, 214110 (2013).
[20] N. A. Smirnov, J. Phys.: Condens. Matter **29**, 105402 (2017).
[21] L. Burakovsky, S. P. Chen, D. L. Preston, and D. G. Sheppard, J. Phys.: Conf. Ser. **500**, 162001 (2014).
[22] S. Anzellini, V. Monteseguro, E. Bandiello, A. Dewaele, L. Burakovsky, and D. Errandonea, Sci. Rep. **9**, 13034 (2019).
[23] V. M. Elkin, V. N. Mikhaylov, A. A. Ovechkin, and N. A. Smirnov, J. Phys.: Condens. Matter **32**, 435403 (2020).
[24] N. A. Smirnov, J. Phys.: Condens. Matter **33**, 035402 (2021).
[25] S. Yu. Savrasov, Phys. Rev. B **54**, 16470 (1996).
[26] O. Gunnarsson and B. Lundqvist, Phys. Rev. B. **13**, 4274 (1976).
[27] J. P. Perdew, J. A. Chevary, S. H. Vosko, K. A. Jackson, M. R. Pederson, D. J. Singh, and C. Fiolhais, Phys. Rev. B. **46**, 6671 (1992); **48**, 4978(E) (1993).
[28] J. P. Perdew, A. Ruzsinszky, G. I. Csonka, O. A. Vydrov, G. E. Scuseria, L. A. Constantin, X. Zhou, and K. Burke, Phys. Rev. Lett. **100**, 136406 (2008).
[29] N. A. Smirnov, Phys. Rev. B **101**, 094103 (2020).
[30] P. E. Blochl, O. Jepsen, and O. K. Andersen, Phys. Rev. B **49**, 16223 (1994).
[31] G. Parsafar and E. A. Mason, Phys. Rev. B **49**, 3049 (1994).
[32] J. Sólyom, *Fundamentals of the Physics of Solids* (Springer, Berlin, 2009), Vol. 1.
[33] Y. Mishin, M. J. Mehl, D. A. Papaconstantopoulos, A. F. Voter, and J. D. Kress, Phys. Rev. B **63**, 224106 (2001).
[34] S. Japel, B. Schwager, R. Boehler, and M. Ross, Phys. Rev. Lett. **95**, 167801 (2005).
[35] J. Akella and G. C. Kennedy, J. Geophys. Res. **76**, 4969 (1971).
[36] D. Errandonea, J. Appl. Phys. **108**, 033517 (2010).
[37] N. A. Smirnov, Phys. Rev. B **97**, 094114 (2018).
[38] B. Grabowski, L. Ismer, T. Hickel, and J. Neugebauer, Phys. Rev. B **79**, 134106 (2009).
[39] O. Hellman, I. A. Abrikosov, and S. I. Simak, Phys. Rev. B **84**, 180301(R) (2011).
[40] O. Hellman, P. Steneteg, I. A. Abrikosov, and S. I. Simak, Phys. Rev. B **87**, 104111 (2013).
[41] I. Errea, M. Calandra, and F. Mauri, Phys. Rev. B **89**, 064302 (2014).
[42] D.-B. Zhang, T. Sun, and R. M. Wentzcovitch, Phys. Rev. Lett. **112**, 058501 (2014).
[43] A. Glensk, B. Grabowski, T. Hickel, and J. Neugebauer, Phys. Rev. Lett. **114**, 195901 (2015).
[44] F. J. Pinski, P. B. Allen, and W. H. Butler, Phys. Rev. B **23**, 5080 (1981).